

Assessing Facial Image Accordance to ISO/ICAO Requirements

R. L. Parente, L. V. Batista
Informatics Center - CI
Federal University of Paraíba - UFPB
João Pessoa, Brazil
rodrigolparente@gmail.com, leonardo@ci.ufpb.br

Igor L. P. Andrezza, Erick V. C. L. Borges,
Rajiv A. T. Mota
VSoft Tecnologia
João Pessoa, PB, Brasil
{igor.andrezza, erick.borges, rajiv.mota}@vsoft.com.br

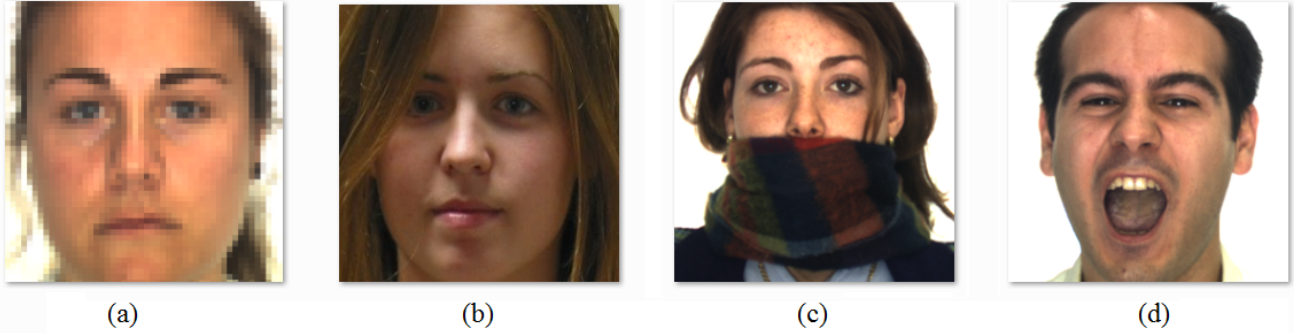


Fig. 1. ICAO requirements studied in this paper: (a) Pixelation, (b) Hair across eyes, (c) Veil Over Face and (d) Mouth Opened.

Abstract—Face has been adopted as default biometric validation method and the International Standard Organization (ISO) proposed a standard which states constraints for facial image. This paper presents methods for evaluating face image conformance to the following ISO/ICAO requirements: pixelation, hair across eyes, veil over face and mouth opened. Each requirement is individually evaluated. The algorithm for analyzing pixelation achieved an equal error rate (EER) equals to 1.7%, result very close to state-of-the-art (0.0% EER). The "Hair Across Eyes" analysis method achieved an EER equals to 11.9% which surpass the best state-of-art result (12.4%). The algorithm for evaluating "Veil Over Face" requirement achieved EER equals to 1.2% which also surpass the best state-of-art result (2.5%). The "Mouth Opened" requirement achieved an EER equals to 4.20%, a result compatible with state-of-art rates for this requirement (3.3%).

Keywords—Face Image quality; ICAO; ISO/IEC 19794-5; Pixelation; Hair across eyes; Veil Over Face; Mouth Opened;

I. INTRODUCTION

Face is a very relevant biometric characteristic which is used in many promising forensic and commercial applications such as access control, video-surveillance, etc. This work focuses on its adoption for electronic identity documents. The International Civil Aviation Organization (ICAO) endorsed, in 2002, the use of face recognition as the globally interoperable biometric characteristic for machine assisted identity confirmation with machine readable travel documents [1]. In sequence, according to ICAO directives, the International Standard Organization (ISO) proposed the ISO/ IEC 19794-5 standard [2], which specifies some quality requirements for facial images.

Between them can be listed: recording format for encoding, recording and transmitting the facial image information, scene constraints, photographic properties, etc. For instance, a face image should not present an opened mouth to be included in an electronic passport. Currently, verifying the compliance of a face image to the ISO/ICAO standard is quite hard task once there are many requirements to verify. This activity is performed in most cases by human experts, with or without automated system support. A complete automation of this task would provide great benefits such as a faster production of the document; unfortunately the experiments carried out in Ferrara *et al.* [3] and Maltoni *et al.* [4] clearly show that the performance of existing commercial products for automatic ISO/ICAO compliance verification are still unsatisfactory.

The objectives of this work are both to propose novel approaches for evaluating the conformance of facial images to some ISO/ICAO requirements and to compare their performance with other proposed methods with published results. The requirements studied in this work are: Image Pixelation, presence of hair across eyes, veil over the face and mouth opened.

This paper is organized as follows: in section II is made a review of the literature related to analysis and segmentation of hair, skin and mouth; the section III introduces the YC_bC_r color model, which is one of most use method for color based skin segmentation; section IV introduces the testing platform, face databases and testing protocol; in section V the proposed algorithms are explained; in section VI the

experiments and results are presented; in section VII the results are discussed and conclusions are presented. Future works are also proposed.

II. RELATED WORKS

As face recognition is becoming a very popular way of biometric validation a new level of facial image constraints is being adopted. The International Standard Organization (ISO) released the ISO/IEC 19794-5 standard, which specifies the record format for encoding, recording and transmitting the facial image information, and defines scene constraints, photographic properties and digital image attributes of facial images. Regarding this context, Ferrara *et al.* [5] present the BioLab-ICAO framework, an evaluation benchmark available to the scientific community, designed to encourage the research on automated ISO/ICAO standards face compliance verification. Approaches for analyzing face image conformance to all ISO/ICAO requirements are proposed. It approaches pixelation requirement by using Prewitt operator [6] to highlight the edges and then Hough lines transform [7] to find straight line segments. The presence of hair in front of the eyes is analyzed by using an improved version of the hair segmentation method proposed by Ferrara *et al.* [8]. The presence of facial occlusion such as veil or scarf is assessed by constructing a skin map as proposed by Storer *et al.* [9]. The "opened mouth" requirement is detected by searching regions related to mouth and teeth. This is accomplished by color analysis, considering pixels belonging to predefined ranges of RGB bands values. It results in mouth and teeth maps which are useful information for mouth state inference.

Rousset *et al.* [10] propose an automatic method for hair segmentation. This method is divided in two steps. Firstly, some information is extracted from frequential and color analysis in order to create binary masks as descriptor of the hair location. Secondly, a matting treatment which is a process to extract foreground object from an image is performed.

Lee *et al.* [11] present an algorithm for hair and face segmentation in 2D images. This approach starts by using learned mixture models of color and location information to suggest the hypotheses of the face, hair, and background regions. In turn, the image gradient information is used to generate the likely suggestions in the neighboring image regions. Either Graph-Cut or Loopy Belief Propagation algorithm is then applied to optimize the resulting Markov network in order to obtain the most likely hair and face segmentation from the background. It is demonstrated that the algorithm can precisely identify the hair and face regions from a large dataset of face images automatically detected by the state-of-the-art face detector.

Min *et al.* [12] explore face recognition in the presence of partial occlusions, with emphasis in occlusions caused by sunglasses and scarf. It first analyzes the presence of potential occlusion on a face and then conducts face recognition on the non-occluded facial regions. The face image is equally divided in two regions: upper and lower parts of the face. The upper part is used for analyzing the presence of sunglasses while the

lower part is used for detecting scarf. The Occlusion detection is performed by generalized Potts model Markov random field (GPM-MRF) proposed by Boykov *et al.* [13].

Min *et al.* [14] approach the occlusion detection problem using Gabor wavelets, PCA and support vector machines (SVM), while the recognition of the non-occluded facial part is performed using block-based local binary patterns. Experiments on AR face database showed that the proposed method yields significant performance improvements compared to existing works for recognizing partially occluded and also non-occluded faces. Furthermore, the performance of the proposed approach is also assessed under illumination and extreme facial expression changes, demonstrating interesting results.

Storer *et al.* [9] present a novel algorithm for occlusion detection and evaluate its performance on several databases. A straight-forward algorithm based on color space techniques which gives a very high performance on this database is presented. The HSV color space is used to model the skin color. This approach is based on automatic color correction and on the H-channel of the HSV color space. Several experiments using different color spaces (RGB, YUV, LAB, YCbCr, etc) were conducted and it has been found that the H-channel (Hue) of the HSV color space is best suited for occlusion detection on facial images. The H-channel image is binarized and some post-processing is applied to remove remaining noise. Masks are defined for the lower part of the face and the eyes to obtain a final value for the level of occlusion.

Ahlvers *et al.* [15], describe a method for tracking face in images presenting head and shoulders. This tracking is based in color information and occurs without model of faces. The segmentation of skin color region is accomplished in YC_bC_r color space, and the component values should simultaneously obey the following conditions: $Y > 80$; $85 < C_b < 135$; $135 < C_r < 180$.

Kim *et al.* [16] propose a face occlusion verification method for an automated teller machine (ATM) application. The proposed method mainly consists of three steps. Firstly, a head and shoulder shape is detected by applying B-spline active contour to motion edges. This motion edge is generated by a kurtosis-based frame selection and distance transformation based motion edge detection. Secondly, a face area is estimated by fitting an ellipse to the detected head and shoulder shape. Finally, occlusion of the face area is determined by measuring skin color area ratio (SCAR) of whole face area and facial component areas.

Hsu *et al.* [17] propose a face detection algorithm for color images in the presence of a varying lighting conditions as well as complex backgrounds. The method uses a novel lighting compensation technique based in YC_bC_r color information aiming to construct skin maps corresponding to eyes, mouth and boundary. Skin detection is performed over the entire image and then face candidates are generated by considering the spatial arrangement of these skin patches. Mouth cluster is calculated according to equation 1:

$$MouthMap = C_r^2 \times \left[C_r^2 + \left(n \times \frac{C_r}{C_b} \right) \right]^2 \quad (1)$$

$$\text{given: } n = 0.95 \times \frac{\sum_{(x,y)} C_r(x,y)^2}{\sum_{(x,y)} \frac{C_b(x,y)}{C_r(x,y)}}.$$

Where:

- C_b is blue chrominance band of YC_bC_r color space;
- C_r is red chrominance band of YC_bC_r color space.

Caplier [18] proposes an algorithm for automatically detecting lip contours in an image sequence. The proposed method does not depend on the speaker and also does not depend on what he is saying. Mouth frames are acquired under natural lighting conditions and make-up or markers are not required. The chosen approach for lip boundaries detection is based on Active Shape Model [19]. Integration of temporal information all over the sequence is done with Kalman filtering, which allows to track mouth shape from frame to frame and provides an initial shape for the lip detection algorithm. At the end of this process the algorithm informs when a transition from closed mouth to opened mouth occurs, and vice-versa.

III. YCBCR COLOR SPACE

According to Chitra *et al.* [20], color space is a mathematical model to represent color information as three or four different color components. Different color models are used for different applications such as computer graphics, image processing, TV broadcasting, and computer vision. There are many color spaces which are useful for the skin detection. They are: RGB based color space (RGB, normalized RGB), Hue Based color space (HSI, HSV, and HSL), Luminance based color space (YCbCr, YIQ, and YUV), and perceptually uniform color space (CIEXYZ, CIELAB, and CIELUV).

The RGB color information presents a lot of redundancy. So, according to Kakumanu *et al.* [21] the orthogonal color spaces reduce the redundancy present in RGB color channels and represent the color with statistically independent components (as independent as possible). The Y value represents the luminance (or brightness) component, computed as a weighted sum of RGB values, the Cr and Cb values, also known as the color difference signals, represent the chrominance component of the image, they are computed by subtracting the luminance component from B and R values. As the luminance and chrominance components are explicitly separated, these spaces are a favorable choice for skin detection, and because of that, YCbCr space is one of the most popular choices for skin analysis. The values of the YC_bC_r components are calculated according to the following equations:

$$\begin{cases} Y = 0.229 \cdot R + 0.587 \cdot G + 0.144 \cdot B \\ Cb = 0.168 \cdot R + 0.3313 \cdot G + 0.5 \cdot B + 128 \\ Cr = 0.5 \cdot R + 0.4187 \cdot G + 0.0813 \cdot B + 128 \end{cases} \quad (2)$$

IV. EVALUATION FRAMEWORK: BIOLAB-ICAO

The BioLab-ICAO framework is a framework developed aiming to provide a common benchmark for the evaluation of algorithms for ICAO compliance verification algorithms to the scientific community through the website[22]. It consists of: 1) a set of requirements, directly derived from the ISO/ICAO standard; 2) a large database of face images and related ground truth data, produced by human experts with a manual labeling process; 3) a testing protocol for objective performance evaluation and comparison; 4) a set of baseline algorithms internally designed to evaluate the compliance to each defined requirement.

Evaluating automatic systems aimed to verify the compliance of face images to the ISO standard requires a large database of images representative of many different possible defects indefied by the defined requirements. To do so, it was used public databases. The database contains 1741 images from the AR database [23], 1935 images from the FRGC database [24], 291 images from the PUT database [25], 804 images artificially generated by applying ink-marked/creased, pixelation and washed-out effects to compliant images from the AR database and 817 newly acquired images. The database is supplied with the ground-truth data, produced by human experts with a manual labeling process, needed for an objective performance evaluation [5].

The testing protocol adopted requires the SDK to yield as an output in the range [0 ... 100] for each requirement, which represents the compliance degree of the image to the requirement. The value 100 indicates that the image is compliant with that requirement and 0 means it is noncompliant. Sometimes an algorithm can fail in processing an image or to evaluate a specific characteristic of the image, therefore, a rejection occurs. The equal error rate (EER) is calculated from the distribution of the degrees of compliance and used to evaluate the performance for each characteristic.

V. METHODS

This section aims to describe the proposed algorithms for each one of the ISO/ICAO requirements addressed in this paper. The individual algorithms proposed here return a compliance degree in the range [0–100], as stated by the used benchmark[5]. Each requirement is introduced and described in details in the subsections ahead.

A. Pixelation

A pixelated image present the characteristic aspect with pixels bigger than normal (Fig. 2). This effect commonly appears after bad quality image resizing to a bigger dimensions. When the image enlargement is done without interpolation, many neighboring pixels present the same value at the same time. This common aspect of pixelated images present well defined edges in both horizontal and vertical directions. According to Ferrara *et al.* [5] an ad hoc method for detecting image pixelation is based in edge detection by Prewitt operator followed by Hough Line transform for line detection. Following this hint, the pixelation detection is performed in similar way.



Fig. 2. Example of pixelated image.

The main steps of the proposed method for pixelation detection are illustrated in image Fig. 3. The input image is converted to grayscale (Fig. 3.a and Fig. 3.d) and Canny edge detection is performed (Fig. 3.b and Fig. 3.e) in the eyes region. Hough Transform [7] for line detection is then performed. If the image is pixelated the result of the edge detection will present several vertical and horizontal lines (Fig. 3.c) which will be detected by Hough lines transform. Otherwise, Hough transform may detect lines in varied directions (Fig. 3.f) according to the eye eyes. Each line is considered vertical or horizontal if its angle is within a predefined tolerance. The score is given by the ratio of the number of lines marked as vertical or horizontal by the total number of lines detected by Hough transform.

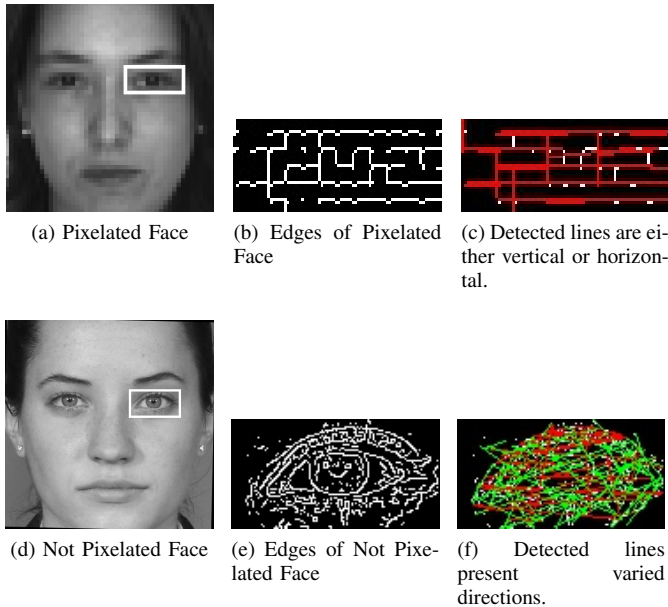


Fig. 3. Steps of Pixelation analysis.

B. Hair Across Eyes

This requirement states that no hair should be in front of the eyes. In order to evaluate this requirement, an algorithm based

on the human face symmetry was developed. Considering that the human face present bilateral symmetry, when the image of right eye is horizontally flipped and overlapped by the image of the left eye the difference between these images should be small. When the image present hair across the eyes, this difference should be greater than when no hair is present.

The main steps of the algorithm are illustrated in Fig. 4 and Fig. 5. These images present the execution of the method for images, respectively, with and without hair in front of the eyes. The first step of the algorithm is to rotate the face, removing the slope between the eyes. The eye pupils are then located and regions of interest (ROI) are calculated for each eye, according to the distance between the eyes (D_{eyes}). The ROI of each eye (Fig. 4.a and Fig. 5.a) correspond to a rectangle with height equals to $D_{eyes}/3$ and width $5D_{eyes}/8$.

The LogAbout filter (proposed by Liu *et al.*[26]) is executed aiming to decrease the influence of light conditions and shadows projected over the face. In the next step, a smoothing operation is performed in order to reduce the remaining noise. Then, Canny edge detection filter [27] is executed in order to detect the edged of the eyes and, possibly, the presence of hair edges as well (Fig. 4.b, Fig. 4.c, Fig. 5.b and Fig. 5.c). A horizontal flip operation is performed in the left eye aiming to fit the right eye (Fig. 4.c and Fig. 5.c). Aiming to join dashed lines and remove noise, the erode and dilate operations are then performed (Fig. 4.d, Fig. 4.e, Fig. 5.d and Fig. 4.e).

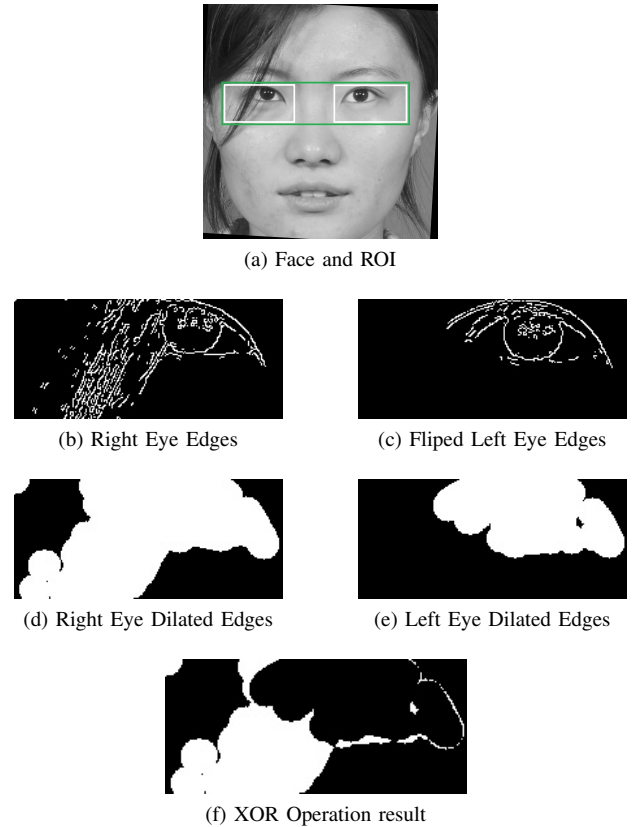


Fig. 4. Hair across eyes processing steps for an image with hair in front of the eyes.



(a) Face and ROI



(b) Right Eye Edges



(c) Fliped Left Eye Edges



(d) Right Eye Dilated Edges



(e) Left Eye Dilated Edges



(f) XOR Operation result

Fig. 5. Hair across eyes processing steps for an image without hair in front of the eyes.

The resulting images of the eyes are compared through a bitwise XOR operation (Fig. 4.f and Fig. 5.f), which highlights the non coincident pixels in the resulting image. The score is obtained as described in Equation 3 and 4.

$$score = \frac{\sum_{j=1}^h \sum_{i=1}^w I_{XOR}(i, j)}{w \cdot h} \quad (3)$$

$$I_{XOR}(i, j) = \begin{cases} 1, & \text{if the pixel belongs to foreground} \\ 0, & \text{otherwise} \end{cases} \quad (4)$$

Where:

- h is the height of the face image;
- w is the width of the face image;
- I_{XOR} is the image resulted from XOR operation.

C. Veil Over Face

Many kinds of face occlusion such as hand covering eyes, sunglasses, scarf, veil, etc, may occur in facial images. The "veil over face" requirement analyzes the presence of occlusions in front of the face, which are not allowed by ISO/ICA0 norms. Skin segmentation has shown to be a very efficient method for facial occlusion detection by veil, scarf, or any other stuff which color is unlike skin color.

Detection of face occlusion by veil or scarf can be performed by simply looking for regions that present non natural

skin tone. The process is illustrated in Fig. 6. The $YCbCr$ color space is used to verify the presence of veil over the face or other kinds of face occlusion. Given the face square region (Fig. 6.a, Fig. 6.d), a skin cluster (Fig. 6.b and Fig. 6.e) of face is calculated by using a modified version of the method proposed by Ahlvers *et al.* [15] but using a narrower interval for the values of Y band. The lower portion of the face (Fig. 6.c and Fig. 6.f) is taken as region of interest.



(a) Face Square Region



(b) Skin Map



(c) ROI - Lower third of the face



(d) Face Square Region



(e) Skin Map



(f) ROI - Lower third of the face

Fig. 6. Veil Over the Face analysis steps for face image with facial occlusion (a)(b)(c) and image without occlusion (d)(e)(f).

The score is calculated by the ratio between the number of pixels marked as skin into the lower part of the face image and the total number of pixels in this region. This calculation is accomplished by using Equations 5 and 6.

$$score = \frac{\sum_{j=1}^h \sum_{i=1}^w Skin(i, j)}{w \cdot h} \quad (5)$$

$$Skin(i, j) = \begin{cases} 1, & \text{if the pixel is marked as skin} \\ 0, & \text{otherwise} \end{cases} \quad (6)$$

Where:

- h is the height of lower part of the face;
- w is the width of lower part of the face;
- $Skin$ is the resulting image of the skin cluster.

D. Mouth Opened

In order to perform the detection of opened mouth, a color based analysis is performed in mouth region. Mouth lips usually present red and teeth present white predominant color tones. The proposed method performs a search for these colors aiming to find lips and teeth. The mouth region (**Mouth_{reg}**) is detected by using the OpenCV [28] cascade classifier and then it is expanded in order to ensure that whole mouth will

be into the region. A smoothing filter is applied in order to reduce noise. After that, the method calculates two measures: the first for mouth detected region (M_{mouth}) and a second one for teeth detection (M_{teeth}).

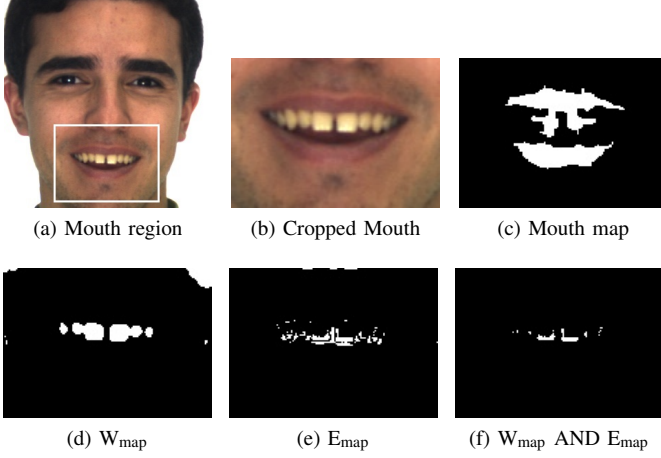


Fig. 7. Opened Mouth detection steps for an image in which the mouth is opened.

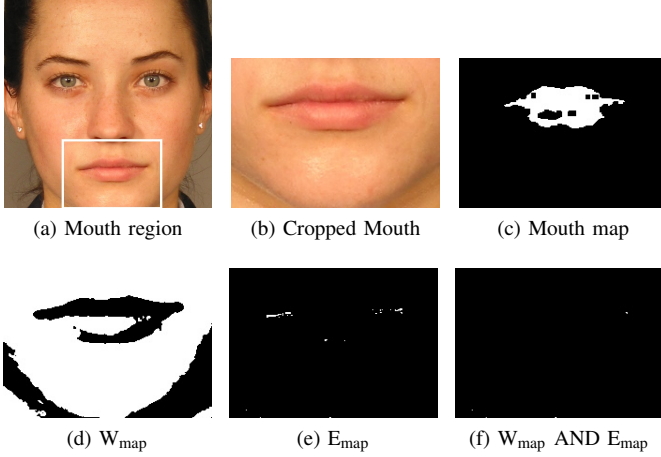


Fig. 8. Opened Mouth detection steps for an image in which the mouth is closed.

Fig. 7 and Fig. 8 illustrate the steps for accomplishing the detection of opened mouth, respectively for an image with mouth opened and another one with mouth closed. The calculation of M_{mouth} starts by constructing a mouth map into the mouth region (Fig. 7.a and Fig. 8.a). It is done by using the method described in Equations 1 and II. This process generates the mouth map (Fig. 7.c and Fig. 8.c), i.e., a binary mask image which foreground corresponds to the mouth. A search is made to find the biggest continuous region and the other regions smaller than 20% of it are marked as background. The height of the mouth map foreground is calculated through the height difference (ΔH) between the foreground pixels with maximum and minimum vertical coordinate. M_{mouth} score is obtained through the quotient of ΔH by the height of **Mouth_{reg}**.

The calculation of M_{teeth} is based in a white pixels mask (W_{map}) and another mask for the edges of teeth (E_{map}). Both maps (Fig. 7.d, Fig. 7.e, Fig. 8.d and Fig. 8.e) are calculated into $Mouth_{reg}$, which is cropped and converted to grayscale. W_{map} is calculated through a threshold operation performed on the gray image that results in a binary mask which foreground correspond to the brighter regions. E_{map} is calculated through the Laplacian filter followed by a threshold operation. This process results in a binary mask which foreground correspond to teeth edges. Finally, W_{map} and E_{map} are merged through a logical AND operation (Fig. 7.f and Fig. 8.f). The final score M_{teeth} is given as described in Equation 7.

$$M_{teeth} = \frac{\sum_{j=1}^h \sum_{i=1}^w (W_{map} \wedge E_{map})(i, j)}{\sum_{j=1}^h \sum_{i=1}^w W_{map}(i, j)} \quad (7)$$

Where:

- h is the height of both W_{map} and E_{map} ;
- w is the width of both W_{map} and E_{map} ;

Once measured the scores for mouth and teeth detection, these are merged and the final score for the mouth opened requirement is obtained according to Equation 8:

$$score = \begin{cases} (M_{mouth} + M_{teeth})/2 & , \text{ if } M_{teeth} \geq T \\ M_{teeth} & , \text{ otherwise} \end{cases} \quad (8)$$

where T is predefined threshold.

VI. EXPERIMENTS AND RESULTS

The proposed methods were tested by using the BioLab-ICAO framework [4] which was developed to provide to the scientific community a common benchmark for the evaluation of algorithms for ICAO compliance verification. Two commercial SDKs (SDK1 and SDK2), whose names cannot be disclosed, and the BioLabSDK were evaluated on through the same framework and have presented their results by Ferrara *et al* [5]. The algorithm BioTest, developed by Biometrika srl, has been also evaluated [29]. Table I presents the EER achieved by the method and the column Reject refers to the images that could not be processed by an SDK.

The proposed method for pixelation detection achieved an EER result which is compatible to the other state-of-the-art methods but it could not be able to surpass them. The EER chart is presented in Fig. 9.a.

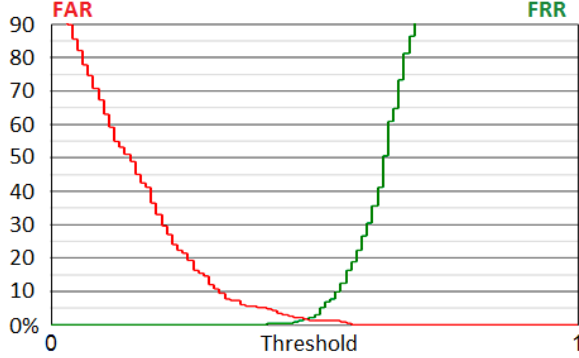
The algorithm that analyzes the compliance for hair across the eyes reached the smaller error rate concerning to the other methods presented in literature. The EER chart for this requirement is presented in Fig. 9.b.

The method of veil detection, as occurred in results for "hair across the eyes", also presented the smaller error rate comparing to the other listed methods. Fig. 9.c presents the EER chart for this requirement.

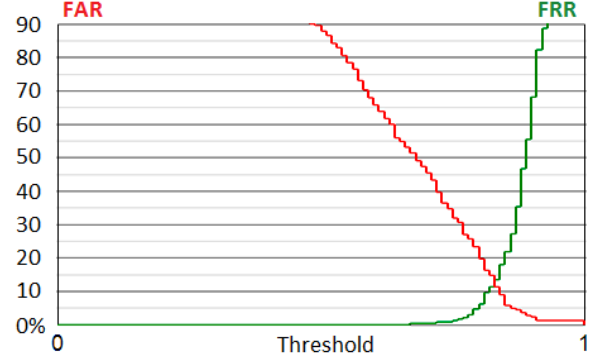
The algorithm that analyzes opened mouth achieved the second-best EER result. The SDK1 framework present ERR

TABLE I
EER AND REJECTION RATE OF THE EVALUATED SDKs

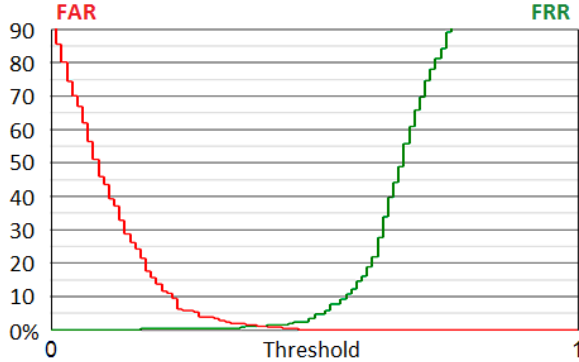
Characteristic	Pixelation		Hair Across Eyes		Veil Over the Face		Opened Mouth	
	EER	Rej.	EER	Rej.	EER	Rej.	EER	Rej.
SDK1	-	-	50.0%	81.9%	-	-	3.3%	52.1%
SDK2	0.0%	0.0%	-	-	-	-	-	-
BioLabSDK	1.3%	0.0%	12.8%	0.0%	2.5%	0.0%	6.2%	0.0%
BioTest	32.4%	0.6%	12.4%	4.6%	3.7%	0.0%	5.0%	2.7%
Proposed Methods	1.7%	0.0%	11.9%	3.4%	1.2%	0.5%	4.2%	0.2%



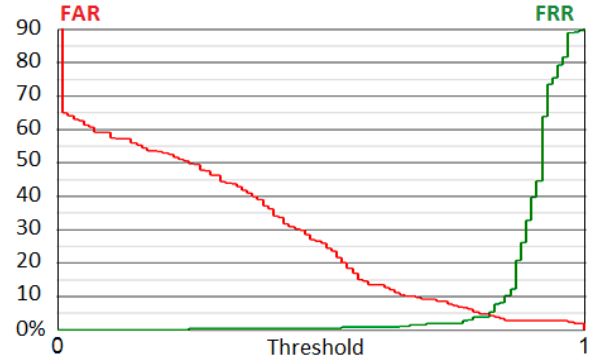
(a) Pixelation



(b) Hair Across Eyes



(c) Veil Over Face



(d) Opened Mouth

Fig. 9. FAR x FRR charts for the evaluated requirements: (a)Pixelation, (b)Hair across eyes, (c) Veil over face and (d)Opened mouth requirements

equals to 3.3% which is better than the result achieved by the proposed mouth verification method. Although, the rejection rate for SDK1 in this requirement is 52.1%, which represents an enormous difference concerning to 0.2% reached by the proposed method for verification of opened mouth. The EER chart for this requirement is presented in Fig. 9.d.

VII. CONCLUSIONS AND FUTURE WORK

This work presented novel approaches for accomplishment of some ISO/ICAO requirements. These are: pixelation, hair across eyes, veil over the face and opened mouth.

The proposed method for pixelation analysis is based on edges detection followed by lines detection through Hough Lines transform. This method was surpassed by SDK2 and

BioLabSDK, although, it achieved an error rate equals to 1.7% which is a comparable result concerning to state-of-the-art methods, showing that the proposed algorithm is an efficient way for verifying the accordance to this requirement.

The proposed algorithm for analyzing the presence of hair across eyes is based on the human face symmetry. The left eye is flipped and compared to right eye. The difference between them is taken as hint to measures the amount of hair in front of the eyes. The proposed method achieved error rate equals to 11.9%, overcoming all the other methods. Although, the EER result bigger than 10% shows that automatically verifying the compliance for this requirement is not an easy task.

In the same way, the method proposed for analysis of veil

over the face is based on skin color segmentation and also surpassed all the other methods present in literature, achieving EER results equal to 1.2%.

The proposed algorithm for detection of opened mouth is based in color segmentation, looking for lips and teeth color tones. This proposed method presented EER equals to 4.2% being surpassed by 3.3% achieved by SDK1. Although, the rejection rate achieved by the proposed method is close to zero, contrasting to 52.1% presented by SDK1. It shows that the proposed method is capable to achieve low EER, rejecting few samples.

As future work, it would be interesting to experiment other skin segmentation methods for those requirements which makes use of it. This enables to evaluate the impact of skin clustering in the proposed methods. It is also interesting to analyze the computational resource consumption, optimizing the processing steps and memory use.

ACKNOWLEDGMENT

The authors thank VSoft and FAPESQ for the sponsorship through the TECNOVA Program. R. L. Parente is sponsored by CAPES.

REFERENCES

- [1] I. N. T. W. Group *et al.*, "Biometrics deployment of machine readable travel documents," 2004.
- [2] "International standard iso/iec jtc 1/sc 37 n506," ISO Technical Committees, Tech. Rep., 2004.
- [3] M. Ferrara, A. Franco, and D. Maltoni, "Evaluating systems assessing face-image compliance with icao/iso standards," in *Biometrics and Identity Management*. Springer, 2008, pp. 191–199.
- [4] D. Maltoni, A. Franco, M. Ferrara, D. Maio, and A. Nardelli, "Biolab-icao: A new benchmark to evaluate applications assessing face image compliance to iso/iec 19794-5 standard," in *ICIP*, 2009, pp. 41–44.
- [5] M. Ferrara, A. Franco, D. Maio, and D. Maltoni, "Face image conformance to iso/icao standards in machine readable travel documents," *Information Forensics and Security, IEEE Transactions on*, vol. 7, no. 4, pp. 1204–1213, 2012.
- [6] R. C. Gonzalez and R. E. Woods, *Digital image processing*. Prentice hall Upper Saddle River, 2002, vol. 3.
- [7] J. Illingworth and J. Kittler, "A survey of the hough transform," *Computer vision, graphics, and image processing*, vol. 44, no. 1, pp. 87–116, 1988.
- [8] M. Ferrara, A. Franco, and D. Maio, "A multi-classifier approach to face image segmentation for travel documents," *Expert Systems with Applications*, vol. 39, no. 9, pp. 8452–8466, 2012.
- [9] M. Storer, M. Urschler, and H. Bischof, "Occlusion detection for icao compliant facial photographs," in *Computer Vision and Pattern Recognition Workshops (CVPRW), 2010 IEEE Computer Society Conference on*. IEEE, 2010, pp. 122–129.
- [10] C. Rousset and P.-Y. Coulon, "Frequent and color analysis for hair mask segmentation," in *Image Processing, 2008. ICIP 2008. 15th IEEE International Conference on*. IEEE, 2008, pp. 2276–2279.
- [11] K.-c. Lee, D. Anguelov, B. Sumengen, and S. B. Gokturk, "Markov random field models for hair and face segmentation," in *Automatic Face & Gesture Recognition, 2008. FG'08. 8th IEEE International Conference on*. IEEE, 2008, pp. 1–6.
- [12] R. Min, A. Hadid, and J.-L. Dugelay, "Efficient detection of occlusion prior to robust face recognition," *The Scientific World Journal*, vol. 2014, 2014.
- [13] Y. Boykov, O. Veksler, and R. Zabih, "Markov random fields with efficient approximations," in *Computer vision and pattern recognition, 1998. Proceedings. 1998 IEEE computer society conference on*. IEEE, 1998, pp. 648–655.
- [14] R. Min, A. Hadid, and J.-L. Dugelay, "Improving the recognition of faces occluded by facial accessories," in *Automatic Face & Gesture Recognition and Workshops (FG 2011), 2011 IEEE International Conference on*. IEEE, 2011, pp. 442–447.
- [15] U. Ahlvers, R. Rajagopalan, and U. Zolzer, "Model-free face detection and head tracking with morphological hole mapping," in *Signal Processing Conference, 2005 13th European*. IEEE, 2005, pp. 1–4.
- [16] G. Kim, J. K. Suhr, H. G. Jung, and J. Kim, "Face occlusion detection by using b-spline active contour and skin color information," in *Control Automation Robotics & Vision (ICARCV), 2010 11th International Conference on*. IEEE, 2010, pp. 627–632.
- [17] R.-L. Hsu, M. Abdel-Mottaleb, and A. K. Jain, "Face detection in color images," *Pattern Analysis and Machine Intelligence, IEEE Transactions on*, vol. 24, no. 5, pp. 696–706, 2002.
- [18] A. Caplier, "Lip detection and tracking," in *Image Analysis and Processing, 2001. Proceedings. 11th International Conference on*. IEEE, 2001, pp. 8–13.
- [19] A. Lanitis, C. J. Taylor, and T. F. Cootes, "Automatic interpretation and coding of face images using flexible models," *Pattern Analysis and Machine Intelligence, IEEE Transactions on*, vol. 19, no. 7, pp. 743–756, 1997.
- [20] S. Chitra and G. Balakrishnan, "Comparative study for two color spaces hsbcr and ycbcr in skin color detection," *Applied Mathematical Sciences*, vol. 6, no. 85, pp. 4229–4238, 2012.
- [21] P. Kakumanu, S. Makrogiannis, and N. Bourbakis, "A survey of skin-color modeling and detection methods," *Pattern recognition*, vol. 40, no. 3, pp. 1106–1122, 2007.
- [22] BioLab, "Biometric system laboratory web site," 2012. [Online]. Available: <https://biolab.csr.unibo.it>
- [23] A. M. Martinez, "The ar face database," *CVC Technical Report*, vol. 24, 1998.
- [24] P. J. Phillips, "Face recognition grand challenge," in *Biometric Consortium Conference*, 2004.
- [25] A. Kasinski, A. Florek, and A. Schmidt, "The put face database," *Image Processing and Communications*, vol. 13, no. 3-4, pp. 59–64, 2008.
- [26] H. Liu, W. Gao, J. Miao, and J. Li, "A novel method to compensate variety of illumination in face detection," in *JCIS*. Citeseer, 2002, pp. 692–695.
- [27] J. Canny, "A computational approach to edge detection," *Pattern Analysis and Machine Intelligence, IEEE Transactions on*, no. 6, pp. 679–698, 1986.
- [28] G. Bradski and A. Kaehler, *Learning OpenCV: Computer vision with the OpenCV library*. "O'Reilly Media, Inc.", 2008.
- [29] BioLab, "Fvc web site," 2006. [Online]. Available: <https://biolab.csr.unibo.it/FvcOnGoing>